



UNIVERSITY OF LEEDS

This is a repository copy of *Temperature dependence of the intrinsic and extrinsic contributions in $\text{BiFeO}_3\text{-(K}_{0.5}\text{Bi}_{0.5})\text{TiO}_3\text{-PbTiO}_3$ piezoelectric ceramics*.

White Rose Research Online URL for this paper:
<https://eprints.whiterose.ac.uk/82879/>

Version: Published Version

Article:

Bennett, TP, Shrout, TR, Zhang, SJ et al. (4 more authors) (2014) Temperature dependence of the intrinsic and extrinsic contributions in $\text{BiFeO}_3\text{-(K}_{0.5}\text{Bi}_{0.5})\text{TiO}_3\text{-PbTiO}_3$ piezoelectric ceramics. *Journal of Applied Physics*, 116 (9). 094102. ISSN 0021-8979

<https://doi.org/10.1063/1.4894443>

Reuse

Items deposited in White Rose Research Online are protected by copyright, with all rights reserved unless indicated otherwise. They may be downloaded and/or printed for private study, or other acts as permitted by national copyright laws. The publisher or other rights holders may allow further reproduction and re-use of the full text version. This is indicated by the licence information on the White Rose Research Online record for the item.

Takedown

If you consider content in White Rose Research Online to be in breach of UK law, please notify us by emailing eprints@whiterose.ac.uk including the URL of the record and the reason for the withdrawal request.



eprints@whiterose.ac.uk
<https://eprints.whiterose.ac.uk/>

Temperature dependence of the intrinsic and extrinsic contributions in BiFeO₃-(K_{0.5}Bi_{0.5})TiO₃-PbTiO₃ piezoelectric ceramics

J. Bennett, T. R. Shrout, S. J. Zhang, P. Mandal, A. J. Bell, T. J. Stevenson, and T. P. Comyn

Citation: *Journal of Applied Physics* **116**, 094102 (2014); doi: 10.1063/1.4894443

View online: <http://dx.doi.org/10.1063/1.4894443>

View Table of Contents: <http://scitation.aip.org/content/aip/journal/jap/116/9?ver=pdfcov>

Published by the AIP Publishing

Articles you may be interested in

[Tailoring the structure and piezoelectric properties of BiFeO₃-\(K_{0.5}Bi_{0.5}\)TiO₃-PbTiO₃ ceramics for high temperature applications](#)

Appl. Phys. Lett. **103**, 152901 (2013); 10.1063/1.4824652

[Phase transitions, relaxor behavior, and large strain response in LiNbO₃-modified Bi_{0.5}\(Na_{0.8}K_{0.2}\)_{0.5}TiO₃ lead-free piezoceramics](#)

J. Appl. Phys. **114**, 044103 (2013); 10.1063/1.4816047

[Effect of composition on electrical properties of lead-free Bi_{0.5}\(Na_{0.8}K_{0.2}\)_{0.5}TiO₃-\(Ba_{0.98}Nd_{0.02}\)TiO₃ piezoelectric ceramics](#)

J. Appl. Phys. **114**, 027005 (2013); 10.1063/1.4811813

[High thermal stability of piezoelectric properties in \(Na_{0.5}Bi_{0.5}TiO₃\)_x-\(BaTiO₃\)_y-\(Na_{0.5}K_{0.5}NbO₃\)_{1-x-y} ceramics](#)

Appl. Phys. Lett. **102**, 012906 (2013); 10.1063/1.4773983

[Piezoelectric and ferroelectric properties of \[Bi_{0.5} \(Na_{1-x-y} K_x Li_y \)_{0.5} \] Ti O₃ lead-free piezoelectric ceramics](#)

Appl. Phys. Lett. **88**, 062901 (2006); 10.1063/1.2171799



SHIMADZU | Excellence in Science | Powerful, Multi-functional UV-Vis-NIR and FTIR Spectrophotometers

Providing the utmost in sensitivity, accuracy and resolution for applications in materials characterization and nano research

- Photovoltaics
- Polymers
- Thin films
- Paints
- Ceramics
- DNA film structures
- Coatings
- Packaging materials

[Click here to learn more](#)



Temperature dependence of the intrinsic and extrinsic contributions in $\text{BiFeO}_3\text{-(K}_{0.5}\text{Bi}_{0.5})\text{TiO}_3\text{-PbTiO}_3$ piezoelectric ceramics

J. Bennett,^{1,a)} T. R. Shrout,² S. J. Zhang,² P. Mandal,³ A. J. Bell,¹ T. J. Stevenson,¹ and T. P. Comyn¹

¹*Institute for Materials Research, School of Process, Environmental and Materials Engineering, University of Leeds, Leeds LS2 9JT, United Kingdom*

²*Materials Research Institute, The Pennsylvania State University, University Park, Pennsylvania 16802, USA*

³*Department of Chemistry, University of Liverpool, Liverpool L69 7ZD, United Kingdom*

(Received 22 July 2014; accepted 20 August 2014; published online 4 September 2014)

This contribution focuses on the use of modified Rayleigh law as a technique for determining the intrinsic and extrinsic (reversible/irreversible) contributions to the piezoelectric effect up to 150 °C across a broad compositional space, augmenting previous understanding of the $\text{BiFeO}_3\text{-(K}_{0.5}\text{Bi}_{0.5})\text{TiO}_3\text{-PbTiO}_3$ system. At room temperature, a mechanistic explanation of the correlation between crystal symmetry, i.e., tetragonal spontaneous strain, x_s , and the Rayleigh relations using Landau theory is provided. The intrinsic response was found to be heavily dependent upon the tetragonal x_s , whereby an optimisation between polarization and permittivity was elucidated, leading to enhanced piezoelectric charge coefficients. A c/a ratio of ~ 1.041 was identified at which the room temperature intrinsic and extrinsic effects were at a maximum; a d_{init} of 183×10^{-12} m/V and Rayleigh coefficient of 59×10^{-18} m²/V² were measured, resulting in the largest piezoelectric charge coefficients. The piezoelectric charge coefficient d_{33} , intrinsic and extrinsic contributions of these materials were all found to increase up to 150 °C while adhering to the Rayleigh model. The reversible extrinsic component of the total reversible response, d_{init} , was calculated to be relatively minor, 4.9% at room temperature, increasing to 12.1% at 150 °C, signifying its increasing influence to the piezoelectric effect, as domain wall motion is thermally activated. Hence, the phenomenological interpretation provided here may be used as a roadmap to elucidate the origins of the temperature dependence of the piezoelectric effect. © 2014 AIP Publishing LLC.

[<http://dx.doi.org/10.1063/1.4894443>]

I. INTRODUCTION

$\text{Pb(Zr}_x\text{Ti}_{1-x})\text{O}_3$ (PZT) ceramics were discovered in 1952¹ and are ubiquitous in piezoelectric sensors, actuators, and transducers.² Their piezoelectric properties are a result of a practically temperature-independent morphotropic phase boundary (MPB) between rhombohedral and tetragonal symmetries; in this region, both the intrinsic and extrinsic contributions to the piezoelectric effect are enhanced.³ PZT undergoes a paraelectric phase transition in the region of 386 °C. $\text{BiFeO}_3\text{-PbTiO}_3$ (BFPT) also displays an MPB, where a Curie temperature (T_C) of 632 °C is observed;⁴ however, piezoelectric coefficients across the compositional space are found to be low, <15 pm/V.⁵ Difficulties with poling these ceramics has led to limited piezoelectric performance across the compositional space with high conductivity largely prohibiting its use at elevated temperatures, and this can often lead to dielectric breakdown. Furthermore, electric-fields in excess of 18 kV/mm can be required for the poling of undoped compositions owed to the high c/a ratio of ~ 1.18 at the MPB.⁶ Lanthanum doping enables the realisation of increased piezoelectric charge coefficients, with a d_{33} of 109 pm/V observed whilst maintaining a T_C of 450 °C for the composition $\text{Bi}_{0.50}\text{Fe}_{0.50}\text{Pb}_{0.47}\text{La}_{0.03}\text{TiO}_{3.015}$. The

extrinsic contribution to the piezoelectric effect was found to be extremely low,⁷ proposed to be a result of ferroelastic domain wall pinning. This effect was also observed by Leist who suggested that a threshold c/a ratio was identified at 1.045, above which the coercive field (E_C) is elevated and domain switching is suppressed.⁸

The recently reported $(1-x-y)\text{BiFeO}_3\text{-}x(\text{K}_{0.5}\text{Bi}_{0.5})\text{TiO}_3\text{-}y\text{PbTiO}_3$ (BF-KBT-PT hereafter) system^{9,10} demonstrated excellent piezoelectric properties compared to BFPT.⁵ The crystal structure of the BF-KBT-PT system was found to vary significantly across the mixed symmetry region (MSR), where a coexistence of rhombohedral and tetragonal symmetries was identified. Increased tetragonality across the MSR was commensurate with increased PbTiO_3 content, which also correlated with a rise in the Curie temperature; however, a trade-off was observed with the piezoelectric activity as demonstrated by reduced d_{33} and k_p values. It was proposed that a number of compositions belonging to the BF-KBT-PT system behave in a similar manner to PZT, although with a higher E_C and T_C , hence the reduced room temperature d_{33} .⁹

Ferroelectric ceramics exhibit both intrinsic and extrinsic contributions to the piezoelectric effect.¹¹ The Rayleigh law was first used to describe induced magnetization and magnetic permeability for low field levels below the coercive magnetic field (H_C).¹² The analogy between ferromagnetic and ferroelectric behavior led to its application in describing

^{a)}Author to whom correspondence should be addressed. Electronic mail: pm07jb@leeds.ac.uk

non-linear dielectric, ferroelectric, and piezoelectric responses^{13,14} and was more recently reapplied.^{15,16} The intrinsic contribution is a result of the atomic displacements of the unit cell under an applied field, whilst the extrinsic contribution is a result of non-180° domain wall motion¹⁷ and is generally associated with irreversible and lossy processes and can greatly affect the electromechanical response. Therefore, as the intrinsic and extrinsic contributions vary with composition and temperature,¹⁸ Rayleigh analysis is an effective method of analysing new materials. Piezoelectric ceramics are often characterised from electrical impedance at low voltage (0.5–1 V) frequency sweeps in conjunction with the sample geometry and density¹⁹ while transducers and actuators are typically driven at much higher excitation levels (1–2 kV/mm).²⁰ This technique therefore allows the possibility of simulated studies of real applications (assuming that the ceramics will not be driven by bipolar switching electric-fields). The technique has been applied to BaTiO₃, PZT, BiScO₃-PbTiO₃, lanthanum doped BFPT, and lead-free materials.^{15,16,18,21–24} Taylor *et al.* expanded upon the use of the Rayleigh model in ferroelectrics to describe the linear dependence of the converse piezoelectric coefficient upon application of an AC electric field.²⁵ The intrinsic response is generally assumed to be independent of the electric-field at low-field amplitudes while non-180° domain wall motion increases the volume fraction to the vector most closely associated with the applied electric-field creating a strain response, thus allowing this behavior to be quantified. The Rayleigh region is restricted to electric field amplitudes that do not cause a change in domain density; these are typically limited to between one-half to one-third of the coercive field.²¹ The principal difficulty with this technique is attaining accurate displacement measurements due to the relatively low fields applied. The piezoelectric Rayleigh coefficient (a_d) can be obtained experimentally with relatively few terms from a plot of d_{33} as a function of maximum field strength

$$d_{33} = d_{init} + \alpha_d \cdot E_0, \quad (1)$$

where d_{init} is a field independent term and represents the contribution from the reversible intrinsic response along with the reversible motion of interfaces and E_0 is the maximum field strength. The term $\alpha_d E_0$ represents contributions to d_{33} from irreversible domain wall translation processes.

The value of the Rayleigh coefficient is a gauge as to the extent of extrinsic domain wall contributions. We obtain the values of the above terms experimentally using the gradient and its extrapolation back to zero field of the d_{33} as a function of E_0 from sub-switching x-E loops. An additional relationship can be used to describe the strain behaviour at any given field amplitude

$$x = (d_{init} + \alpha_d E_0)E \pm \frac{\alpha_d}{2} (E_0^2 - E^2), \quad (2)$$

where x is the strain and E is the instantaneous electric field. This can be used to confirm that the experimental results adhere to the Rayleigh law.

The fractional contribution to the piezoelectric effect from irreversible extrinsic contributions at $E_0 = 1$ kV/mm can be estimated using the following equation:

$$\begin{aligned} &\text{Extrinsic contribution} \\ &= \frac{d_{extrinsic}}{d_{intrinsic} + d_{extrinsic}} = \frac{\alpha_d \cdot E_0}{d_{init} + \alpha_d \cdot E_0}. \end{aligned} \quad (3)$$

As stated previously, the intrinsic effect is dominated by distortions of the lattice and a contribution from domain wall vibrations is also possible, which are reversible and relatively non-lossy at room temperature.²¹ The temperature dependence of the intrinsic piezoelectric response can be approximated using Landau theory^{26,27} in single crystal, bulk polycrystalline, and thin films using the following equation:

$$d = 2\epsilon_r \epsilon_0 \sqrt{Q} x_s, \quad (4)$$

where ϵ_r and ϵ_0 are the relative permittivity and free-space permittivity respectively, Q is the electrostrictive coefficient, and x_s is the tetragonal spontaneous strain, which can be related to the spontaneous polarization

$$P_s = \sqrt{\frac{x_s}{Q}}. \quad (5)$$

Q is assumed to be largely temperature independent.^{28,29} This equation can be used to explain the effect of tetragonal spontaneous strain upon the intrinsic response and the origin of the high-temperature intrinsic behaviour.

Due to the large tetragonality across the MSR in the BF-KBT-PT system, it is assumed that the piezoelectric Rayleigh coefficient, α_d , will also be much reduced compared to other canonical ferroelectrics materials identified in the literature.³⁰ The objective of this study was to analyse the intrinsic and extrinsic contributions of ceramics belonging to the BF-KBT-PT family as a function of temperature to augment the understanding of this system. The materials characterized all reside within the MSR and were chosen as they exhibited reasonable piezoelectric charge coefficients, 152–228 pC/N, coupled with Curie temperatures in excess of PZT, 410–514 °C.

II. EXPERIMENTAL

Ceramics belonging to the compositions shown in Table I were produced using a solid-state reaction method. Each composition has been assigned a letter for ease of identification and discussion. Samples were produced from powders of the commercially available Bi₂O₃ (99.9%), PbO (99.9%), Fe₂O₃ (99%), TiO₂ (99.9%), and K₂CO₃ (99+%) (Sigma-Aldrich). Stoichiometric mixtures of the starting reagents were attrition milled using a Dyno-mill KDL Type-A (Willy A. Bachofen, Switzerland) with yttria-stabilized zirconia (YSZ) (Tosoh, Japan) beads in propan-2-ol for 0.5 h. Dried and sieved powders were then calcined at 800 °C for 4 h in air. Subsequently, 1 wt. % Glascol HA-40 binder (Allied Colloids, UK) was added and mixed. Powders were uniaxially pressed at 50 MPa in order to form pellets, followed by cold isostatic pressing at 300 MPa for 10 min to increase the green density of the unsintered pellets. The binder was burnt out by slow heating to

TABLE I. Summary of electrical properties and Rayleigh parameters at room temperature for BF-KBT-PT, La-BFPT,⁷ and PZT^{45,46} ceramics, the d_{33} values were measured using a Berlincourt meter, the E_C was taken from x-E data at 7 kV/mm.

Composition	A	B	C	D	E	La-BFPT	PZT
(1-x-y) BiFeO ₃	0.584	0.566	0.556	0.537	0.562		
x(K _{0.5} Bi _{0.5})TiO ₃	0.131	0.169	0.188	0.225	0.225		
yPbTiO ₃	0.285	0.265	0.256	0.238	0.213		
d_{33} (pC/N)	152	206	228	220	203	120	180
E_C (kV/mm)	4.21	3.93	3.64	3.98	4.01	10	-
T_C	514	442	427	419	410	450	386
Tetragonality (c/a)	1.061	1.045	1.041	1.034	1.25	-	-
$\alpha_d \times 10^{-18}$ (m ² /V ²)	23	42	59	51	38	4.2	130
$d_{\text{init}} \times 10^{-12}$ (m/V)	128	76	183	179	170	82.4	242.4
Extrinsic cont. (%)	15.1	19.4	24.3	22.2	18.4	4.8	~25

600 °C, followed by sintering at 1050–1065 °C for 2 h in a covered crucible therefore reducing the loss of volatile elements such as lead, bismuth, and potassium.³¹ Pellets were then mechanically lapped to <1 mm, ensuring that the sample was flat across the entire surface to enable accurate measurements and electroded with a fire-on (550 °C) conductive silver paste (Gwent Group, UK). Poled samples were required for Rayleigh analysis. Further analysis on poled samples was performed using a number of techniques as a function of temperature, namely, permittivity, thermally stimulated depolarization current (TSDC) measurements, and x-ray diffraction. These experiments were performed more than 24 h after poling to allow the samples to age appropriately as discussed by Eitel and Randall.¹⁷

In order to record the electric-field induced strain (x-E) measurements at 1 Hz, a linear variable differential transducer (LVDT) was used in line with a DSP SR830 lock-in amplifier (Stanford Research, USA) and a high voltage TREK 610C power supply (TREK, USA). A National Instruments data acquisition card was used to record the data. Samples were placed in an oil bath with the LVDT fixture suspended in a convection furnace. The temperature was recorded at the sample using a thermocouple and samples were held at the set temperature for 10 min before measurements commenced. Low temperature measurements were carried out before high temperature measurements. Relative permittivity was measured at 1 kHz as a function of temperature using an Agilent 4192A, with a non-inductively wound furnace upon heating using a ramp rate of 2 °C/min. TSDC measurements were performed using a Keithley 6430 to measure current as a function of time. A constant heating rate dT/dt of 2 °C/min was used following Anton *et al.*³² X-ray diffraction (Cu K α_1) was performed on highly polished samples; this was achieved using up to 1 μ m diamond suspensions with proprietary polishing cloths (Buehler, UK) in order to reduce the significance of surface effects.

III. RESULTS

A. Measurement of the Rayleigh response

All materials characterized exhibited the perovskite structure with no discernible impurity phases detected. A

phase coexistence between rhombohedral and tetragonal symmetries was established in agreement with previous publication.¹⁰ The tetragonality and Curie temperature scale with the PbTiO₃ content while the piezoelectric charge coefficient d_{33} did not as shown in Figure 1. The optimal poling conditions based upon a study of varying electric-field, time, and temperatures were used; this regime involved an applied electric-field of 6–7 kV/mm at 75–100 °C for 10 min in order to fully pole the samples.

All the compositions studied demonstrated a linear relationship between the d_{33} as a function of the amplitude of the applied electric-field between $0.2 < E_0 < 1$ kV/mm. An example of the data collected is showcased in Figure 2(a). The piezoelectric coefficient d_{33} of each composition increased with electric-field and temperature, which is consistent with the literature.¹⁷ The piezoelectric d_{33} observed remained linear up to 150 °C, which signifies adherence to the Rayleigh model as it is only applicable in the linear region. It can also be inferred that the samples were fully poled and new domains were not nucleated during the measurement.²¹ The maximum applied field is generally $\sim 1/4$ of the E_C at 25 °C. This threshold field reduces as anticipated with increased temperature and is $\sim 1/3$ of the coercive field at 150 °C, identified from electric-field induced strain measurements at 7 kV/mm and 0.1 Hz that are not presented in this contribution. Figure 2(b) illustrates the measured and calculated electric-field induced strain loops at 25 °C and 150 °C in order to verify that the Rayleigh model was applicable to this system at both room and high temperatures. Reasonable agreement was found across all compositions between the measured and calculated loops at both 25 °C and 150 °C with opening of the loops evident at elevated temperatures as anticipated, and no major asymmetric hysteresis was observed that is characteristically associated with hard materials or piezoelectric switching. Composition E shows the greatest divergence from the calculated strain and the amount of loss had been undervalued possibly due to the existence of other hysteretic mechanisms, such as a linear viscoelastic response;^{33,34} however, the divergence was relatively small. Certain piezoelectric materials such as “hard” PZTs deviate from the Rayleigh model as pinning centres are not randomly distributed and an internal bias field forms.⁸

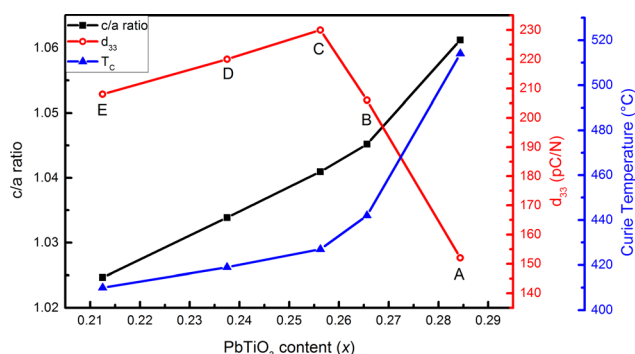


FIG. 1. The c/a ratio, Curie temperature, and d_{33} of the compositions were examined. The stoichiometric ratios of these compositions are shown in Table I.

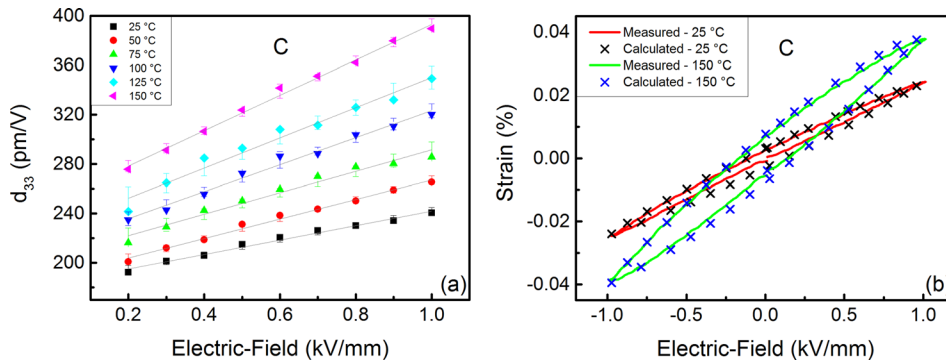


FIG. 2. (a) d_{33} vs. E_0 and (b) measured and calculated electric-field induced strain loops at 25 °C and 150 °C with a maximum field of 1 kV/mm for composition C. Error bars indicate 95% confidence bands from a linear regression.

IV. DISCUSSION

A. The effect of tetragonal distortion on the room-temperature Rayleigh coefficient

In this section, only the room temperature intrinsic/extrinsic piezoelectric response shall be considered, which will be correlated with the tetragonal distortion across the compositional space. The d_{init} was found to be optimised in composition C; the intrinsic component to the piezoelectric effect was found to be 183×10^{-12} (m/V); and the lowest value observed was found in composition A, which displayed the largest tetragonality across the compositional space studied. The largest room temperature Rayleigh coefficient recorded in this study also belonged to composition C. A value of 59×10^{-18} m^2/V^2 was measured, and this was commensurate with the largest piezoelectric coefficient d_{33} of 228 pC/N, with a general decrease in both d_{init} and α_d noted flanking this composition. While the Rayleigh coefficient may be at a maximum in composition C, this trend is mirrored for the E_C , with the lowest value of 3.64 kV/mm observed in composition C, and this increased gradually in the flanking compositions with the largest value being found for composition A, 4.21 kV/mm, commensurate with the tetragonality, demonstrating the importance of domain wall mobility.

The d_{init} , α_d , and fractional irreversible extrinsic contribution values as a function of the c/a ratio are presented in Figures 3(a)–3(c). A clear trend exists between the room temperature d_{init} and the c/a ratio. This correlation holds for the Rayleigh coefficient and total extrinsic contributions although the significance is reduced. An optimum c/a ratio of 1.041 exists in the mixed phase region belonging to composition C, where both the intrinsic and d_{init} and α_d are optimized, with the fractional contribution to the extrinsic piezoelectric effect also enhanced in this composition. This enhancement may be due to proximity to the MPB, as observed in BSPT and PZT as the domain wall density and mobility increases due to the increased number of polarization vectors. When this system is compared to similar piezoelectric compounds such as La-doped BFPT, it is apparent that both the intrinsic and extrinsic contributions have been greatly enhanced as evidenced by the d_{33} , d_{init} , and α_d coefficients. For composition C, the Rayleigh coefficient increased by more than one order of magnitude while the intrinsic contribution more than doubled with respect to BFPT, summarized in Table I, believed to be a result of the reduced tetragonality. Stresses that arise during the paraelectric phase transition to the tetragonal phase in La-

BFPT ceramics, especially those with a high c/a ratio, have been shown to dominate the domain switching behavior as ferroelastic domain walls are pinned. A threshold c/a ratio of 1.045 was suggested with which our findings concur;⁸ above this, domain switching is largely inhibited. This was demonstrated by piezoelectric and electromechanical coupling coefficients in a previous contribution.¹⁰

The explanation for an optimum c/a ratio can be related appropriately to Eqs. (4) and (5); an assumption is made that the electrostriction coefficient is generally independent of perovskite symmetry and the degree of ferroelectric ordering across the compositional space and is largely dependent on cation disorder.²⁸ First, it has been observed using *ab initio* studies³⁵ that increased polarization values correlate strongly with higher experimentally observed $c/a-1$ values for a large number of PbTiO_3 -derived perovskite solutions. Polarization is therefore often reduced in compositions with reduced tetragonal distortions. This behavior is

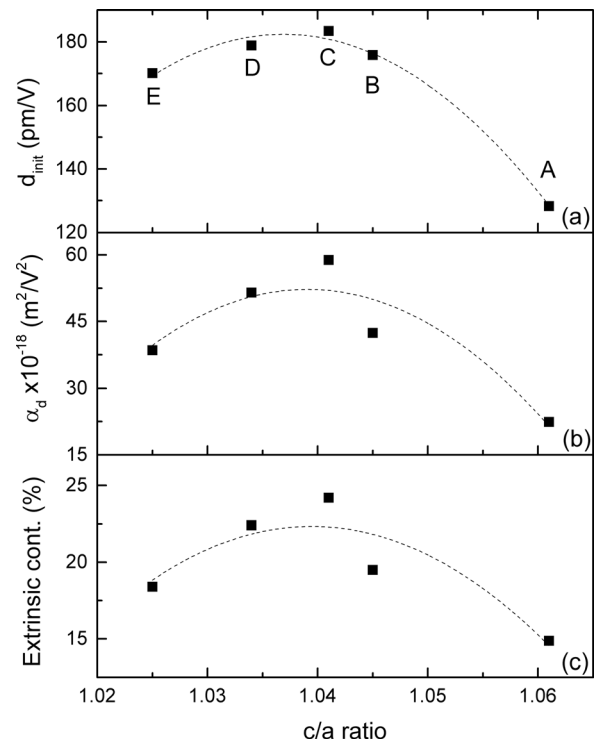


FIG. 3. Room temperature values of the (a) d_{init} , (b) Rayleigh coefficient, α_d , and (c) extrinsic contributions as a function of the tetragonal distortion. The lines are drawn as a guide for the eye.

closely associated with B-site displacement as opposed to A-site displacement in the unit cell; hence, solid solutions with large B-site cations such as BiInO₃ can generate enhanced tetragonality when partially substituted with PbTiO₃.³⁶ Compositions with a high *c/a* ratio often suffer from relatively low relative permittivity values. Composition A (*c/a* = 1.061) has a relative permittivity at room temperature $\epsilon_r = 635$. Conversely, compositions with a low *c/a* ratio demonstrate a considerable increase in the relative permittivity, and composition E with a *c/a* = 1.025 has a relative permittivity $\epsilon_r = 941$. This is also shown in La-BFPT with a significant increase in compositions with a reduced *c/a* ratio.⁸

The Rayleigh response displays a weaker correlation although behaves similarly to d_{init} with an optimum response observed in the same composition; this is not always the case such as in the $\text{Li}_x(\text{Na}_{0.5}\text{K}_{0.5})_{1-x}\text{NbO}_3$ system. The orthorhombic (*Amm2*) and monoclinic (*Pm*) phase exhibited the largest extrinsic contributions while the largest intrinsic contributions were found at the polymorphic phase boundary between the monoclinic and tetragonal (*P4mm*) phase.²³ As stated previously, domain switching can be limited in the tetragonal phase due to the internal mechanical stress. A large lattice distortion and volume phase fraction of the tetragonal phase in mixed symmetry materials may be indicative of a large potential for extrinsic contributions; however, in a pure tetragonal material, for example, the actual response is reduced due to mechanical stress induced upon actuation, as there is a considerable energy barrier preventing non-180° domain switching. In order to fully exploit the potential piezoelectric properties of materials with a large tetragonal lattice distortion, an increase in the rhombohedral phase volume fraction is often useful in order to promote domain switching as the barrier to domain switching is therefore reduced. In PZT, the lattice distortion of the tetragonal phase is reduced, which allows a greater degree of poling. Therefore, a significant volume of the rhombohedral phase is desired in allowing the movement of non-180° domain walls. Kungl suggested that in PZT, a 25%–40% rhombohedral phase is optimum,³⁷ whilst in the BF-KBT-PT system—where the *c/a* ratio (=1.025–1.061) is generally far larger in the mixed symmetry region (cf. *c/a* for La-doped PZT = 1.028)³⁸—a higher rhombohedral content is advantageous. The rhombohedral phase fraction in compositions A–E is between 44% and 71%, while it is 51.2% in composition A, which exhibits a *c/a* ratio of 1.061, thus increasing domain switching compared to the closely related BFPT system.

Additional influencing factors to consider with the reduction of PbTiO₃ content may be due to an increase in localized effects associated with the partial substitution of (K_{0.5}Bi_{0.5})TiO₃ (KBT), which leads to the frustration of the tetragonal ordering due to the reduced tetragonal distortion. Due to the volatility of both the K and Bi cation, vacancies may also lead to pinning of the domains, thus limiting switching. It has also been suggested in the lead-free BiFeO₃-(K_{0.5}Bi_{0.5})TiO₃ system that polar nano-regions may exist. In the BF-KBT-PT system, it is possible that with reduced PbTiO₃ and increased (K_{0.5}Bi_{0.5})TiO₃ content that an increase in the lattice disorder occurs, which reduces the

long-range polar order, thus reducing domain wall energy and resulting in the existence of polar nano-regions.

It has been shown that an optimum *c/a* ratio exists and a trade-off between the lattice polarization and permittivity occurs for the intrinsic effect, this trend is also recorded for the extrinsic effect although the trade-off exists here between potential for domain switching of the respective phases and the saturation of the piezoelectric effect when subjected to an applied electric-field during poling.

B. Origin of the intrinsic/extrinsic response at elevated temperatures

Figures 4(a)–4(e) demonstrate the temperature dependence of the d_{init} and Rayleigh coefficient as extracted from Figure 2(a). Both the α_d and d_{init} increase in magnitude as a function of temperature, which is due to a softening of both reversible intrinsic and irreversible extrinsic contributions. The thermodynamic origin of the enhancement can be owed to the flattening of a free energy profile,³⁹ as the energy required to cause local atomic displacements is lowered and the process of domain switching is thermally activated.¹⁷ d_{init} values demonstrated an approximately linear increase with temperature although the significance of this was much reduced across the compositional space with a reduced amount of PbTiO₃. The lowest d_{init} values observed belonged to composition A, which also demonstrated the lowest increase as a function of temperature from 128–157 × 10⁻¹² m/V. This material possesses the largest tetragonal distortion of all the compositions and also demonstrates the greatest temperature stability. It is noteworthy that composition E exhibited the largest observable d_{33} at 150 °C, while also exhibiting the largest d_{init} value of 268 × 10⁻¹² m/V, the Rayleigh coefficient was modest at 143 × 10⁻¹⁸ m²/V², suggesting that the intrinsic response is critical to an enhanced d_{33} not just in this composition but across the BF-KBT-PT system; thus, the large piezoelectric coefficient in composition E is predominantly due to the displacement of the unit cell—this was the case for all of the compositions studied.

Results indicate that generally a linear trend is found for the Rayleigh coefficient as a function of temperature across all compositions with no discontinuities observed. The Rayleigh coefficient identified for composition A demonstrated the greatest temperature stability, however, this was also the composition with the lowest Rayleigh coefficients of 23 and 73 × 10⁻¹⁸ m²/V² at 25 °C and 150 °C, respectively. This composition has the highest PbTiO₃ content and tetragonality of the compositions presented as well as the lowest room temperature piezoelectric coefficients. The divergence from a linear regression of the Rayleigh coefficient as a function of temperature became more significant with reduced PbTiO₃, and at elevated temperatures in excess of 100 °C. The significant increase in the d_{init} and Rayleigh coefficients in the PbTiO₃-reduced compositions is owed to the lower ferroelectric transition temperatures, T_C , of these compositions.

The fractional irreversible extrinsic contributions to the piezoelectric effect as a function of temperature were calculated using Eq. (3) and are shown in Figures 4(f)–4(j). The

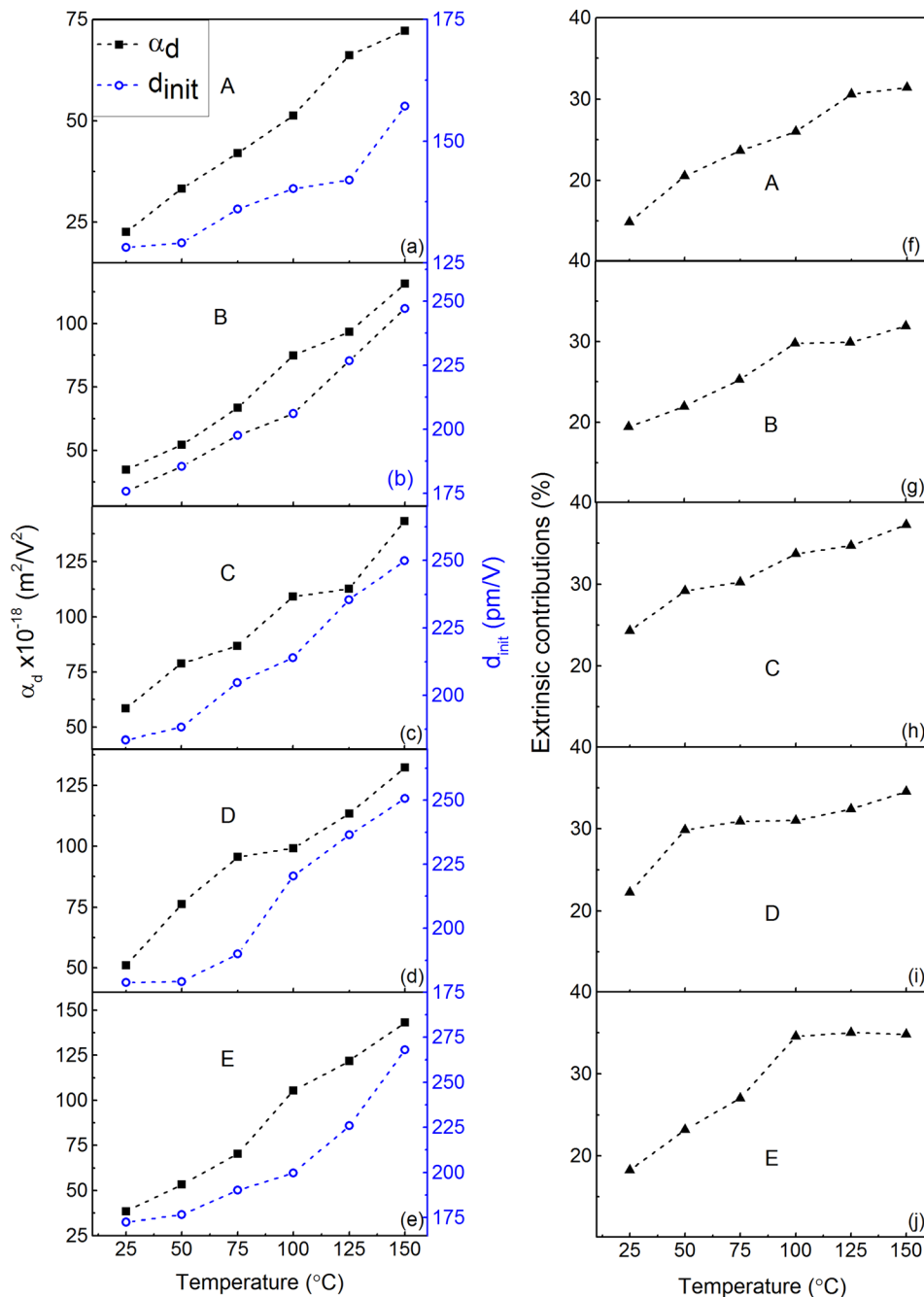


FIG. 4. (a)–(e) the Rayleigh coefficient, α_d , and the d_{init} and (f)–(j).

fractional irreversible extrinsic contributions were found to increase in magnitude as a function of temperature across all of the compositions. This behaviour was also relatively linear in compositions A–C; however, compositions D and E displayed decreasing linearity of the extrinsic contributions, largely due to reduction in the increase of the Rayleigh coefficient, thus confirming that larger tetragonal distortion is associated with greater temperature stability. A similar range of extrinsic contributions was found at room temperature, 15.1%–24.3%, compared to at 150 $^{\circ}\text{C}$, 31.8%–39.6%.

C. Reconstructing the temperature dependence of the intrinsic/extrinsic response

In order to fully understand the enhancement in the intrinsic and extrinsic contributions to the piezoelectric

effect as a function of temperature shown previously, a number of experiments were performed to satisfy the terms presented in Eqs. (4) and (5), to describe the behaviour shown in Figure 4(c) for composition C. Permittivity, polarization, and x-ray diffraction responses were measured as a function of temperature. The electrostriction coefficient was measured at room temperature and was assumed to be temperature independent as observed elsewhere.^{28,29}

The first point to consider is that while the relative permittivity can display an intrinsic and extrinsic component, the applied fields used during this measurement (0.0005 kV/mm) are not significant enough to result in the measurement of the irreversible extrinsic response. Hall suggested that 0.01 kV/mm and 0.3 kV/mm were required to exceed the threshold field, E_t , in a soft and well-aged hard PZT, respectively, below which the permittivity is independent of the

field amplitude, E_0 .¹⁶ A measurement frequency of 1 kHz was selected as conductivity is reduced compared to much lower measuring frequencies. One method that can qualify the intrinsic and extrinsic components of the dielectric nonlinearity is by “freezing out” domain wall contributions by measuring the permittivity at close to 0 K or at extremely high frequencies where the effects of domains are negligible; however, neither of these techniques were available to the author. The relative permittivity displayed a significant temperature dependence; this behaviour was linear up to $\sim 100^\circ\text{C}$, at which point a slight divergence was found. The polarization (although this was not the intrinsic polarisation) determined by TSDC was found to decrease slightly in the temperature range examined as anticipated, shown in Figure 5(b). In contradiction to the electric-field induced polarisation as a function of temperature data often reported in the literature. Although not presented here for the BF-KBT-PT system, at 1 and 7 kV/mm, respectively, an increase was also found, this is proposed to be due to conductivity, while conductivity does not influence the TSDC result. The room temperature effective electrostrictive coefficient, Q_{33} , was derived from the slope of $x\text{-P}^2$ profiles. An average room temperature electrostrictive coefficient, Q_{33} , of $0.0305 \text{ m}^4/\text{C}^2$ was calculated for composition C. Although not presented, the product of the permittivity and polarisation increases up to 150°C , highlighting the dominating effect of the permittivity, thus endorsing the measured d_{init} values presented in Figure 4(c).

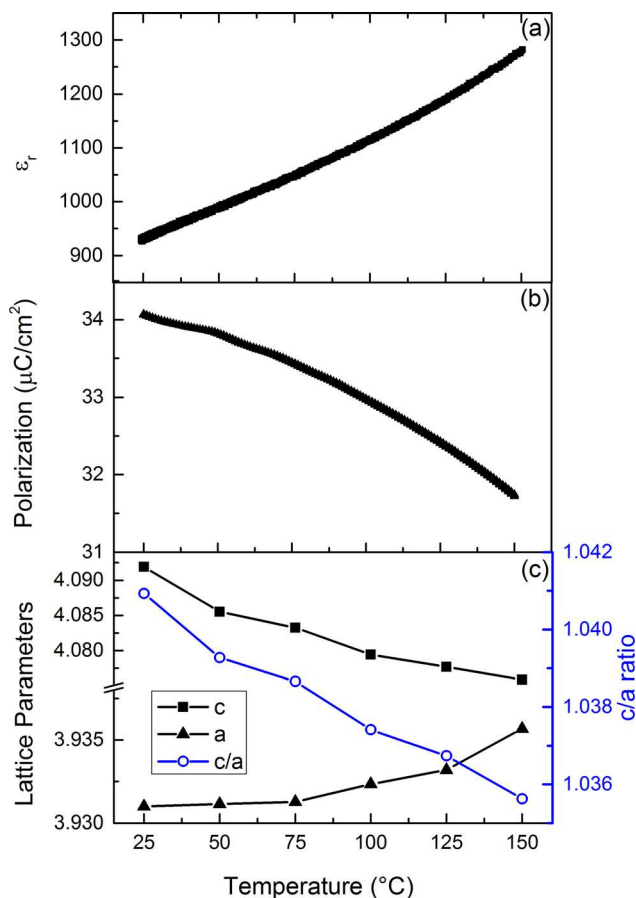


FIG. 5. (a) Relative permittivity, (b) polarization, and (c) lattice parameters of a poled sample as a function of temperature for composition C.

The data presented in Figure 5(c) demonstrate that with increasing temperature a relatively small shift is observed in the a-lattice parameter in contrast to the c-lattice parameter, which experiences a significant reduction; hence, a reduction in the tetragonality (c/a) is observed, accordingly demonstrating the potential for enhanced domain wall mobility. A relatively minor increase (5.5%) in the tetragonal phase volume fraction was observed across the temperature range, which is less significant in the enhancement of piezoelectric properties. The reduction of the tetragonal lattice distortion is commensurate with an associated decrease in internal stress levels.⁸ The linear decrease in the c/a ratio corresponds to the linear increase in the extrinsic response at these temperatures although there is no reason to suggest that this should be the case across different systems or even different compositions of the same system. At high temperatures, the domain wall energy is reduced and domain wall mobility is enhanced, evidenced by the reduction in the electrical coercive-field measured using the converse effect at high-fields (7 kV/mm); this was found to decrease across all compositions as a function of temperature.⁴⁰ As stated previously, the applied electric-field during the Rayleigh measurement was kept at reduced levels well below the coercive field in order to avoid the depolarisation of the sample and nucleation of new domains. The enhancement in both the intrinsic and extrinsic contributions to the piezoelectric coefficient d_{31} has been shown in a previous contribution using resonance analysis, therefore confirming this effect at low and moderate excitation levels.¹⁰

It was therefore possible to calculate the d_{init} and contrast this to the measured d_{init} values. The reversible extrinsic component was calculated by deducting the calculated from the measured values; the results of this are shown in Figure 6. A general increase in the reversible extrinsic contributions was identified with increasing temperature from 9.2 pm/V to 30.2 pm/V at room temperature and 150°C , respectively. An increase in the reversible Rayleigh coefficients has also been demonstrated at the MPB in lead-free piezoelectric ceramics⁴¹ and as a function of temperature in PbTiO_3 -derived thin films.⁴²

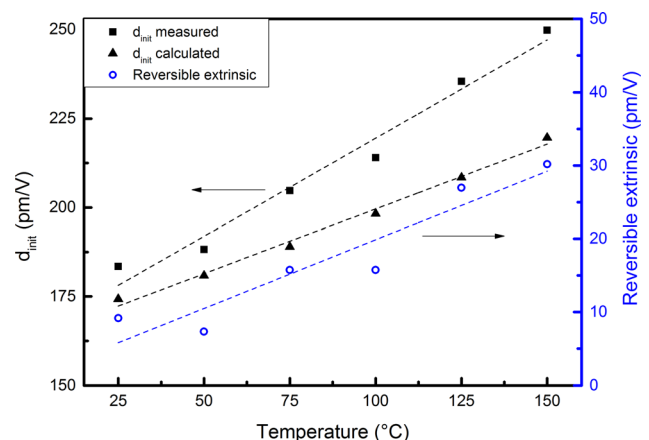


FIG. 6. The measured d_{init} , calculated d_{init} values, and the reversible extrinsic component as a function of temperature for composition C. Linear fits have been included as a guide.

The reversible extrinsic component from domain wall switching that is independent of the applied electric-field strength is often assumed to be relatively minor compared to the reversible intrinsic due to atomic displacements and irreversible extrinsic contributions.⁴³ However, it has been suggested that in hard PZTs that reversible domain wall movement is the dominant mechanism at room temperature as the material response does not adhere to Rayleigh law.⁴⁴ As the Rayleigh law is closely obeyed in the BF-KBT-PT system, it can be inferred that this system behaves more similarly to a soft PZT although driven at much higher excitation levels where lossy processes could become more prevalent, hence an increase in the contribution from reversible domain wall processes.

An increase in the reversible extrinsic components is anticipated with an increase in temperature and can be explained succinctly in terms of the potential energy profile. At room temperature, there is not sufficient thermal energy for extensive polarisation rotation and the reversible motion of interfaces. Potential energy wells at room temperature are significant enough to act as pinning centers as the activation energy required is greater than the thermal energy of the system, kT , required to enable irreversible domain wall switching. As the temperature is increased, the thermal energy increases, thus allowing a greater contribution from irreversible and reversible extrinsic domain wall effects (as they are thermally activated process). The energy barrier also reduces (i.e., the energy potential wells reduce in magnitude and broaden); therefore, for the same excitation levels, an increase in both irreversible and reversible domain wall motion is observed (hence the increase in d_{33} here and d_{31} as a function of temperature shown in a previous contribution¹⁰). The caveat being that the tetragonal spontaneous strain, x_s , lessens as temperature increases therefore reducing the magnitude of these effects. However, the increase in thermal energy and reduction in the energy barrier are dominant in the temperature range discussed.

V. CONCLUSION

In summary, BF-KBT-PT ceramics have been fabricated belonging to the mixed symmetry region between rhombohedral and tetragonal symmetries. Rayleigh analysis was adopted in order to gauge the intrinsic and extrinsic contributions to the piezoelectric effect, as a function of c/a ratio and temperature up to 150 °C. Compared to La-doped BFPT, in the optimum composition, the Rayleigh coefficient, α_d , was increased by more than one order of magnitude ($59 \times 10^{-18} \text{ m}^2/\text{V}^2$) while the intrinsic contribution more than doubled ($183 \times 10^{-12} \text{ m/V}$). This is believed to be owed to the reduced tetragonality, 1.041, while the fractional extrinsic contributions of 24.2% were comparable to that of an undoped PZT. The origin of this optimum composition was explained using simple Landau theory.

An increase in the d_{init} , α_d , and fractional extrinsic contributions was identified up to 150 °C across all compositions while still adhering to the Rayleigh law. The intrinsic and extrinsic contributions of the PbTiO_3 -reduced compositions were significantly enhanced at high temperatures due to their

proximity to the ferroelectric T_C . The intrinsic and extrinsic contributions to the piezoelectric effect were reconstructed and evidenced that at elevated temperatures the reversible extrinsic component is significant with an increase from 9.2 to 30.2 pm/V between 25 °C and 150 °C, respectively. As the measuring temperature is increased, the thermal energy of the system also increases whilst the energy barrier reduces, thus allowing a greater contribution from irreversible and reversible extrinsic domain wall effects.

This study also demonstrates the utility of the BF-KBT-PT ternary system. Similar studies have been performed on La-doped BFPT although La has a considerable impact upon the T_C reducing it to levels below that of PZT, making it redundant as a high temperature piezoceramic. BF-KBT-PT ceramics allow for tailoring of the tetragonal spontaneous strain, x_s , which scales with the PbTiO_3 concentration while not greatly affecting the T_C , ergo, a mechanistic approach can be taken when analysing the reversible intrinsic and the reversible/irreversible extrinsic contributions to the piezoelectric effect. Therefore, this work is of importance to both academia and industry as it provides a useful roadmap for analysing established and novel piezoceramics, particularly materials belonging to ternary systems that adhere to the modified Rayleigh law.

ACKNOWLEDGMENTS

This research has been supported by an EPSRC DTA (EP/P505593/1) and Ionix Advanced Technologies (www.ionix.at). Jeff Long generously granted technical assistance at the Pennsylvania State University.

¹G. Shirane and A. Takeda, "Phase transitions in solid solutions of PbZrO_3 and PbTiO_3 (I) small concentrations of PbTiO_3 ," *J. Phys. Soc. Jpn.* **7**(1), 5–11 (1952).

²R. C. Turner, P. A. Fuieler, R. E. Newnham, and T. R. Shrout, "Materials for high temperature acoustic and vibration sensors: A review," *Appl. Acoust.* **41**(4), 299–324 (1994).

³C. A. Randall, N. Kim, J.-P. Kucera, W. Cao, and T. R. Shrout, "Intrinsic and extrinsic size effects in fine-grained morphotropic-phase-boundary lead zirconate titanate ceramics," *J. Am. Ceram. Soc.* **81**(3), 677–688, (1998).

⁴V. V. S. Sai Sunder, A. Halliyal, and A. M. Umarji, "Investigation of tetragonal distortion in the (PbTiO_3)-(BiFeO_3) system by high-temperature x-ray diffraction," *J. Mater. Res.* **10**, 1301–1306 (1995).

⁵T. P. Comyn, T. Stevenson, and A. J. Bell, "Piezoelectric properties of BiFeO_3 - PbTiO_3 ceramics," in *Applications of Ferroelectrics, 2004, 14th IEEE International Symposium on ISAF-04* (2004), pp. 122–125.

⁶T. P. Comyn, T. Stevenson, and A. J. Bell, "Piezoelectric properties of BiFeO_3 - PbTiO_3 ceramics," *J. Phys. IV France* **128**, 13–17 (2005).

⁷T. P. Comyn and A. J. Bell, "Study of intrinsic/extrinsic piezoelectric contributions in La-doped BiFeO_3 - PbTiO_3 ceramics using the Rayleigh method," in *16th IEEE International Symposium on Application of Ferroelectrics* (2007), Vols. 1–2, pp. 402–403.

⁸T. Leist, T. Granzow, W. Jo, and J. Rodel, "Effect of tetragonal distortion on ferroelectric domain switching: A case study on La-doped BiFeO_3 - PbTiO_3 ceramics," *J. Appl. Phys.* **108**(1), 14103–14106 (2010).

⁹J. Bennett, A. J. Bell, T. J. Stevenson, and T. P. Comyn, "Exceptionally large piezoelectric strains in BiFeO_3 -($\text{K}_0.5\text{Bi}_0.5$) TiO_3 - PbTiO_3 ceramics," *Scr. Mater.* **68**(7), 491–494 (2013).

¹⁰J. Bennett, A. J. Bell, T. J. Stevenson, and T. P. Comyn, "Tailoring the structure and piezoelectric properties of BiFeO_3 -($\text{K}_0.5\text{Bi}_0.5$) TiO_3 - PbTiO_3 ceramics for high temperature applications," *Appl. Phys. Lett.* **103**(15), 152901 (2013).

¹¹S. Li, W. Cao, and L. E. Cross, "The extrinsic nature of nonlinear behavior observed in lead zirconate titanate ferroelectric ceramic," *J. Appl. Phys.* **69**(10), 7219–7224 (1991).

- ¹²L. Rayleigh, "On the behaviour of iron and steel under the operation of feeble magnetic forces," *Phil. Mag.* **23**, 225–245 (1887).
- ¹³A. V. Turik, "Theory of polarization and hysteresis of ferroelectrics," *Phys. Solid State* **5**, 885–887 (1963).
- ¹⁴A. V. Turik, "A statistical method for the investigation of repolarization processes in ferroelectric ceramics," *Phys. Solid State* **5**, 1751–1753 (1964).
- ¹⁵D. Damjanovic and M. Demartin, "The Rayleigh law in piezoelectric ceramics," *J. Phys. D: Appl. Phys.* **29**(7), 2057 (1996).
- ¹⁶D. A. Hall, "Nonlinearity in piezoelectric ceramics," *J. Mater. Sci.* **36**(19), 4575 (2001).
- ¹⁷R. E. Eitel and C. A. Randall, "Octahedral tilt-suppression of ferroelectric domain wall dynamics and the associated piezoelectric activity in Pb(Zr,Ti)O₃," *Phys. Rev. B* **75**(9), 94106 (2007).
- ¹⁸D. Damjanovic and M. Demartin, "Contribution of the irreversible displacement of domain walls to the piezoelectric effect in barium titanate and lead zirconate titanate ceramics," *J. Phys. Condens. Mat.* **9**(23), 4943 (1997).
- ¹⁹A. Petošić, M. Budimir, and N. Pavlović, "Comparison between piezoelectric material properties obtained by using low-voltage magnitude frequency sweeping and high-level short impulse signals," *Ultrasonics* **53**(6), 1192–1199 (2013).
- ²⁰K. H. Gilchrist, D. E. Dausch, and S. Grego, "Electromechanical performance of piezoelectric scanning mirrors for medical endoscopy," *Sens. Actuators A* **178**(0), 193–201 (2012).
- ²¹R. E. Eitel, T. R. Shrout, and C. A. Randall, "Nonlinear contributions to the dielectric permittivity and converse piezoelectric coefficient in piezoelectric ceramics," *J. Appl. Phys.* **99**(12), 124110–124117 (2006).
- ²²S. W. Gotmare, S. O. Leontsev, and R. E. Eitel, "Thermal degradation and aging of high-temperature piezoelectric ceramics," *J. Am. Ceram. Soc.* **93**(7), 1965–1969 (2010).
- ²³K. Kobayashi, Y. Mizuno, K. Hatano, and C. A. Randall, "Rayleigh behavior in the lead free piezoelectric lix(Na_{0.5}K_{0.5})_{1-x}NbO₃ ceramic," *Appl. Phys. Express* **5**(3), 31501 (2012).
- ²⁴B. Peng, Z. Yue, and L. Li, "Evaluation of domain wall motion during polymorphic phase transition in (K, Na)NbO₃-based piezoelectric ceramics by nonlinear response measurements," *J. Appl. Phys.* **109**(5), 054107 (2011).
- ²⁵D. V. Taylor, D. Damjanovic, and N. Setter, "Nonlinear contributions to dielectric and piezoelectric properties in lead zirconate titanate thin films," *Ferroelectrics* **224**(1), 299–306 (1999).
- ²⁶A. L. Kholkin, E. L. Colla, A. K. Tagantsev, D. V. Taylor, and N. Setter, "Fatigue of piezoelectric properties in Pb(Zr,Ti)O₃ films," *Appl. Phys. Lett.* **68**(18), 2577–2579 (1996).
- ²⁷Q. M. Zhang, H. Wang, N. Kim, and L. E. Cross, "Direct evaluation of domain-wall and intrinsic contributions to the dielectric and piezoelectric response and their temperature dependence on lead zirconate-titanate ceramics," *J. Appl. Phys.* **75**(1), 454–459 (1994).
- ²⁸K. Uchino, S. Nomura, L. E. Cross, R. E. Newnham, and S. J. Jang, "Electrostrictive effect in perovskites and its transducer applications," *J. Mater. Sci.* **16**(3), 569–578 (1981).
- ²⁹F. Li, L. Jin, Z. Xu, and S. Zhang, "Electrostrictive effect in ferroelectrics: An alternative approach to improve piezoelectricity," *Appl. Phys. Rev.* **1**(1), 011103 (2014).
- ³⁰A. Pramanick, D. Damjanovic, J. E. Daniels, J. C. Nino, and J. L. Jones, "Origins of electro-mechanical coupling in polycrystalline ferroelectrics during subcoercive electrical loading," *J. Am. Ceram. Soc.* **94**(2), 293–309 (2011).
- ³¹Y. Hiruma, H. Nagata, and T. Takenaka, "Phase diagrams and electrical properties of (Bi_{1/2}Na_{1/2})TiO₃-based solid solutions," *J. Appl. Phys.* **104**(12), 124106 (2008).
- ³²E.-M. Anton, W. Jo, D. Damjanovic, and J. Rodel, "Determination of depolarization temperature of (Bi_{1/2}Na_{1/2})TiO₃-based lead-free piezoceramics," *J. Appl. Phys.* **110**(9), 94108–94114 (2011).
- ³³D. A. Hall and P. J. Stevenson, "High field dielectric behaviour of ferroelectric ceramics," *Ferroelectrics* **228**(1), 139–158 (1999).
- ³⁴F. Li, S. Zhang, Z. Xu, X. Wei, J. Luo, and T. R. Shrout, "Composition and phase dependence of the intrinsic and extrinsic piezoelectric activity of domain engineered (1-x)Pb(Mg_{1/3}Nb_{2/3})O₃-xPbTiO₃ crystals," *J. Appl. Phys.* **108**(3), 034106 (2010).
- ³⁵T. Qi, I. Grinberg, and A. M. Rappe, "Correlations between tetragonality, polarization, and ionic displacement in PbTiO₃-derived ferroelectric perovskite solid solutions," *Phys. Rev. B* **82**(13), 134113 (2010).
- ³⁶S. Zhang, R. Xia, C. A. Randall, T. R. Shrout, R. Duan, and R. F. Speyer, "Dielectric and piezoelectric properties of niobium-modified BiInO₃-PbTiO₃ perovskite ceramics with high Curie temperatures," *J. Mater. Res.* **20**(8), 2067–2071 (2005).
- ³⁷H. Kungl and M. J. Hoffmann, "Temperature dependence of poling strain and strain under high electric fields in LaSr-doped morphotropic PZT and its relation to changes in structural characteristics," *Acta Mater.* **55**(17), 5780–5791 (2007).
- ³⁸M. Hammer, C. Monty, A. Endriss, and M. J. Hoffmann, "Correlation between surface texture and chemical composition in undoped, hard, and soft piezoelectric PZT ceramics," *J. Am. Ceram. Soc.* **81**(3), 721–724 (1998).
- ³⁹M. Budimir, D. Damjanovic, and N. Setter, "Qualitative distinction in enhancement of the piezoelectric response in PbTiO₃ in proximity of coercive fields: 90° versus 180° switching," *J. Appl. Phys.* **101**(10), 104119 (2007).
- ⁴⁰D. Wang, Y. Fotinich, and G. P. Carman, "Influence of temperature on the electromechanical and fatigue behavior of piezoelectric ceramics," *J. Appl. Phys.* **83**(10), 5342–5350 (1998).
- ⁴¹J. Gao, X. Hu, L. Zhang, F. Li, L. Zhang, Y. Wang, Y. Hao, L. Zhong, and X. Ren, "Major contributor to the large piezoelectric response in (1-x)Ba(Zr_{0.2}Ti_{0.8})O₃-x(Ba_{0.7}Ca_{0.3})TiO₃ ceramics: Domain wall motion," *Appl. Phys. Lett.* **104**(25), 252909 (2014).
- ⁴²N. Bassiri-Gharb, I. Fujii, E. Hong, S. Trolier-McKinstry, D. Taylor, and D. Damjanovic, "Domain wall contributions to the properties of piezoelectric thin films," *J. Electroceramics* **19**(1), 49–67 (2007).
- ⁴³M. Davis, D. Damjanovic, and N. Setter, "Temperature dependence of the direct piezoelectric effect in relaxor-ferroelectric single crystals: Intrinsic and extrinsic contributions," *J. Appl. Phys.* **100**(8), 084103 (2006).
- ⁴⁴J. E. Garcia, D. A. Ochoa, V. Gomis, J. A. Eiras, and R. Pérez, "Evidence of temperature dependent domain wall dynamics in hard lead zirconate titanate piezoceramics," *J. Appl. Phys.* **112**(1), 014113 (2012).
- ⁴⁵B. Jaffe and W. R. Cook, *Piezoelectric Ceramics* (Academic Press, London, 1971), Vol. 3.
- ⁴⁶A. Pramanick, D. Damjanovic, J. C. Nino, and J. L. Jones, "Subcoercive cyclic electrical loading of lead zirconate titanate ceramics I: Nonlinearities and losses in the converse piezoelectric effect," *J. Am. Ceram. Soc.* **92**(10), 2291–2299 (2009).